Journal of Data Science 0 (0), 1–21
July 2025
DOI: 10.6339/25-JDS1182
Data Science in Action

Bayesian Multivariate Joint Modeling of Longitudinal, Recurrent, and Competing Risk Terminal Events in Patients with Chronic Kidney Disease

Qi Qian[1], Danh V. Nguyen[2], Esra Kurum[3], Sudipto Banerjee[1], Connie M. Rhee[4,5], and Damla Senturk[1,*]

[1]*Department of Biostatistics, University of California, Los Angeles, CA 90095, USA*
[2]*Department of Medicine, University of California, Irvine, CA 92868, USA*
[3]*Department of Statistics, University of California, Riverside, CA 92521, USA*
[4]*Department of Medicine, University of California, Los Angeles, CA 90095, USA*
[5]*USA and Nephrology Section, VA Greater Los Angeles Health Care System, Los Angeles, CA 90073, USA*

Abstract

Approximately 15% of adults in the United States (U.S.) are afflicted with chronic kidney disease (CKD). For CKD patients, the progressive decline of kidney function is intricately related to hospitalizations due to cardiovascular disease and eventual "terminal" events, such as kidney failure and mortality. To unravel the mechanisms underlying the disease dynamics of these interdependent processes, including identifying influential risk factors, as well as tailoring decision-making to individual patient needs, we develop a novel Bayesian multivariate joint model for the intercorrelated outcomes of kidney function (as measured by longitudinal estimated glomerular filtration rate), recurrent cardiovascular events, and competing-risk terminal events of kidney failure and death. The proposed joint modeling approach not only facilitates the exploration of risk factors associated with each outcome, but also allows dynamic updates of cumulative incidence probabilities for each competing risk for future subjects based on their basic characteristics and a combined history of longitudinal measurements and recurrent events. We propose efficient and flexible estimation and prediction procedures within a Bayesian framework employing Markov Chain Monte Carlo methods. The predictive performance of our model is assessed through dynamic area under the receiver operating characteristic curves and the expected Brier score. We demonstrate the efficacy of the proposed methodology through extensive simulations. Proposed methodology is applied to data from the Chronic Renal Insufficiency Cohort study established by the National Institute of Diabetes and Digestive and Kidney Diseases to address the rising epidemic of CKD in the U.S.

Keywords *competing risks; dynamic prediction; longitudinal data; predictive modeling; survival analysis*

1 Introduction

Chronic kidney disease (CKD), defined by having an estimated glomerular filtration rate (eGFR) less than 60 ml/min/1.73m^2 or a urine albumin-to-creatinine ratio of 30 mg/g or higher, affects

*Corresponding author. Email: dsenturk@ucla.edu.

Received October 1, 2024; Accepted March 28, 2025

more than 1 in 7 U.S. adults (USRDS, 2022). In addition, as of 2020, end-stage kidney disease (ESKD), the final stage of CKD, impacted almost 808, 000 individuals in the U.S., with patients typically dependent on the life-sustaining treatment of dialysis for the duration of their lives or until kidney transplantation. Recent studies have highlighted a significant association between reduced eGFR and increased risk of mortality, cardiovascular (CV) events, and hospitalization among CKD patients (Go et al., 2004). Moreover, individuals with ESKD undergoing hemodialysis exhibit an even higher prevalence of cardiovascular disease (CVD), at about 77% (USRDS, 2022). As a leading cause of mortality, morbidity and frequent hospitalizations, CKD poses a considerable economic burden which escalates substantially with increasing disease severity (Go et al., 2004). Hence, there exists an urgent imperative to develop an effective monitoring tool for CKD progression, along with modeling of interdependent outcomes, recurrent CV hospitalizations and multiple terminal events (ESKD and death), and associated risk factors.

To gain deeper insights into the risk factors that influence the progression of CKD and CVD, as well as the associated morbidity and mortality in CKD patients, the National Institute of Diabetes and Digestive and Kidney Diseases (NIDDK) established the Chronic Renal Insufficiency Cohort (CRIC) study in 2001 (Feldman et al., 2003). This ongoing prospective cohort study recruits adult patients who are aged 21 to 74 years old with mild to moderate CKD. Inspired by the broad aims of the CRIC study, we introduce a novel Bayesian multivariate joint model (BM-JM), designed to study the interdependent dynamics of CKD progression defined by longitudinal eGFR trajectories, recurrent hospitalizations due to CV events, and competing-risk terminal outcomes of ESKD and death. The proposed BM-JM also facilitates dynamic prediction of survival probabilities of each competing-risk terminal outcome for future subjects based on comprehensive individual data, including baseline characteristics, a complete history of previous longitudinal eGFR measurements and past recurrent CV events. Note that even though ESKD or kidney failure may not strictly qualify as a "terminal" event in clinical terms, it is commonly modeled as a survival outcome in the nephrology literature (Yang et al., 2014). Since the longitudinal follow-up of eGFR ends upon the occurrence of ESKD (defined as the initiation of dialysis or kidney transplant) in the CRIC study, it is also treated as a competing risk in our BM-JM modeling.

Methodological development and clinical applications for joint modeling have grown substantially over the past two decades, as extensively reviewed in Lawrence Gould et al. (2015). A commonly used approach to induce dependency among the multiple outcomes modeled is the inclusion of shared frailty/random effects terms (Wulfsohn and Tsiatis, 1997). While most of the literature is on modeling of a continuous longitudinal outcome and a right-censored event time, the joint modeling has been extended to handle interval- (Gueorguieva et al., 2012) and left-censored (Thiébaut et al., 2005) data, discrete event times (Albert and Shih, 2010), competing risks (Williamson et al., 2008), and recurrent event times (Ren et al., 2021). The extension of joint models to accommodate multiple event time outcomes is particularly valuable in health research and clinical decision-making, as patients may often experience multiple, recurrent, or a succession of clinical events (e.g. recurrent CV-related hospitalizations in the CKD population).

Another important extension is the use of joint modeling for dynamic prediction of survival probabilities, based on all available baseline characteristics, longitudinal and/or recurrent events data. Dynamic predictions offer personalized forecasts that can be continuously updated as additional longitudinal and/or recurrent events data become available. Instead of the conventional dependency formulation through random effects, recent literature on dynamic prediction methods include direct longitudinal biomarker effects in the survival submodel (Rizopoulos, 2011). This approach allows for the direct evaluation of the predictive value of longitudinal biomarker

measurements, while also enhancing the accuracy of the dynamic predictions.

Despite important extensions in recent years, existing literature on joint modeling of longitudinal measurements and multiple event time outcomes that include both recurrent and terminal events, remains limited. The literature includes a joint model of (i) CD4 cell counts, intensity of opportunistic disease, and death in patients with HIV (Liu and Huang, 2009); (ii) tumor size, occurrence of new lesions, and death in patients with metastatic colorectal cancer (Król et al., 2016); and (iii) eGFR trajectories, recurrent CV events and a composite terminal event (ESKD or death) in CKD patients (Kürüm et al., 2024). All three models utilize shared random effects to account for the interdependency among the trivariate outcomes, and are limited to a single terminal event outcome.

To address the existing modeling gaps in multivariate joint modeling of longitudinal trajectories, recurrent events and competing-risk terminal events as well as developing an efficient dynamic prediction procedure for competing-risk terminal outcomes utilizing the combined history of longitudinal measurements and recurrent events, we propose a novel Bayesian multivariate joint model (BM-JM). By explicitly modeling the effects of longitudinal biomarker in the competing-risk survival submodels, the proposed BM-JM allows for direct quantification and interpretation of the predictive value of the longitudinal measurements on competing-risk terminal outcomes, while also enabling more precise and comprehensive dynamic predictions for future patients. The proposed framework allows for prediction of each competing risk individually, utilizing the most recent available history of not only longitudinal measurements but also recurrent events. Note that while our data application illustrates the proposed model for longitudinal, recurrent, and two competing-risk terminal processes, the BM-JM framework can be extended to accommodate more complex interdependent multi-disease applications.

The remainder of the paper is organized as follows. Details of the proposed BM-JM, including the proposed estimation and inference procedures, are outlined in Section 2. Section 3 introduces the proposed individualized dynamic prediction framework as well as metrics for evaluating predictive accuracy. Application of the proposed methodology to the CRIC study for joint modeling of kidney function decline, recurrent CV events, and competing-risk terminal events (ESKD and death) for patients with CKD is given in Section 4. Comprehensive simulations to study the finite sample properties of the proposed BM-JM, including its predictive performance are outlined in Section 5. In both the CRIC data application and the simulation studies, the proposed BM-JM is compared with three marginal models (i.e., the longitudinal model (L-M), the recurrent model (R-M), and the competing-risk terminal model (T-M)) and two simplified joint models (i.e., the joint model of longitudinal measurements and competing-risk terminal events (LT-JM) and the joint model of recurrent and competing-risk terminal events (RT-JM)). These comparative analyses reveal that ignoring either recurrent events or longitudinal measurements in joint modeling adversely impacts both parameter inference and predictive performance. We conclude with a brief discussion of key findings and potential future works in Section 6.

2 Proposed Bayesian Multivariate Joint Model (BM-JM)

2.1 Model Specification

Chronic kidney disease (CKD) is commonly defined based on eGFR, which serves as a widely accepted measure of kidney function (Go et al., 2004). Therefore, eGFR measurements are chosen as the longitudinal biomarker in our data application. Let $Y_i(t)$ denote the value of the longitudinal biomarker (i.e., eGFR trajectory) for the ith subject ($i = 1, \ldots, n$) at time t. The

vector of longitudinal measurements, $\mathbf{Y}_i = \{Y_i(t_{i1}), \ldots, Y_i(t_{iK_i})\}^{\mathsf{T}}$, is observed at subject-specific time points t_{ik}, $k = 1, \ldots, K_i$. The true but unobserved values of the longitudinal biomarker over time are denoted by $\xi_i(t)$. A linear structure for $\xi_i(t)$ was selected as it is a common practice in kidney disease modeling. Longitudinal studies have consistently demonstrated that eGFR trajectories typically decline linearly in CKD patients, allowing linear models to effectively estimate both the rate of decline and its clinical significance (Coresh et al., 2007; Skupien et al., 2016). Additionally, adopting a linear structure for $\xi_i(t)$ ensures simplicity and enhances interpretability within the joint modeling framework.

Patients with reduced kidney function face significantly higher risks of mortality and kidney failure compared to the general population (Consortium et al., 2010). Consequently, ESKD and mortality are commonly used as time-to-event outcomes in kidney disease studies (Yang et al., 2014; Fine and Gray, 1999; Grams et al., 2013). In the CRIC study, longitudinal follow-up of eGFR terminates at either ESKD or death, making these two outcomes competing-risk terminal events. Let $T_i^{*(w)}$ $(w = 1, \ldots, W)$ denote the true failure time for the wth competing terminal event for subject i, and C_i the censoring time. For simplicity, $W = 2$ is used in our developments, corresponding to ESKD and death, although the proposed framework can be extended to accommodate multiple competing risk terminal events ($W \geqslant 3$). The observed terminal event time, T_i, is defined as the minimum of the true failure times and the potential censoring time C_i, i.e., $T_i = \min(T_i^{*(1)}, T_i^{*(2)}, C_i)$, with the event indicator δ_i taking values of 0, 1, or 2 to denote censoring, ESKD and death, respectively.

CKD is also a recognized risk factor for recurrent CV events (Consortium et al., 2010), which can exacerbate renal insufficiency and increase mortality risk for CKD patients (Muntner et al., 2002). For the recurrent event processes (e.g., recurrent CV events in our data application), let G_{ij}^* denote the jth true gap time, defined as the time between recurrent events $j-1$ and j. Further let $R_{ij}^* = G_{i1}^* + \cdots + G_{ij}^*$ denote the true total time from the study onset to event j, and let $C_{ij} = C_i - R_{i,j-1}^*$ denote the jth gap censoring time for $j = 1, \ldots, J_i$, with J_i denoting the total number of recurrent events of subject i before censoring. The observed gap time and recurrent event indicator are then defined as $G_{ij} = \min(G_{ij}^*, C_{ij})$ and $\lambda_{ij} = I_{(G_{ij} \leqslant C_{ij})}$, respectively, with $I_{(\cdot)}$ denoting the indicator function.

Several studies have employed joint models to explore the interdependency among longitudinal eGFR measurements, recurrent CV events, and terminal outcomes, such as ESKD and death, in CKD patients. For example, Hillege et al. (2006) utilized joint models to study the relationship between eGFR decline and CV event outcomes in this population. More recently, Kürüm et al. (2024) introduced a Bayesian trivariate model that integrates longitudinal kidney disease progression, recurrent CV events, and a composite terminal event to examine their interrelationships. Despite these advances, existing models exhibit certain limitations. They often do not fully account for competing-risk terminal processes or provide tools for dynamically predicting terminal outcomes using the combined history of longitudinal eGFR trajectories and recurrent CV events. To address these gaps, we propose the BM-JM, a Bayesian joint model that integrates longitudinal eGFR measurements, recurrent CV events, and competing-risk terminal events. The BM-JM explicitly captures the interrelationships among these processes and facilitates dynamic prediction of survival probabilities for both ESKD and death in new patients by incorporating their updated longitudinal and recurrent event profiles. The specific formulation

of the proposed BM-JM is detailed below:

$$\begin{aligned} Y_i(t) &= \xi_i(t) + \varepsilon_i(t) = \mathbf{X}_i^\top \boldsymbol{\beta}_\ell + \mathbf{Z}_i^\top \boldsymbol{\phi}_\ell + \gamma t + b_{i0} + b_{i1} t + \varepsilon_i(t), \\ r_{ij}(g_{ij}) &= h_{r0}(g_{ij}) \exp\left(\mathbf{X}_i^\top \boldsymbol{\beta}_r + \mathbf{Z}_i^\top \boldsymbol{\phi}_{rj} + \sum_{m=0}^{j-1} \alpha_m + \eta_{r0} b_{i0} + \eta_{r1} b_{i1} + \nu_i \right), \\ h_i^{(1)}(t) &= h_{t0}^{(1)}(t) \exp\left(\mathbf{X}_i^\top \boldsymbol{\beta}_t^{(1)} + \mathbf{Z}_i^\top \boldsymbol{\phi}_t^{(1)} + \eta_t^{(1)} \xi_i(t) + \zeta^{(1)} \nu_i \right), \\ h_i^{(2)}(t) &= h_{t0}^{(2)}(t) \exp\left(\mathbf{X}_i^\top \boldsymbol{\beta}_t^{(2)} + \mathbf{Z}_i^\top \boldsymbol{\phi}_t^{(2)} + \eta_t^{(2)} \xi_i(t) + \zeta^{(2)} \nu_i \right), \end{aligned} \tag{1}$$

where $Y_i(t)$, $r_{ij}(g_{ij})$ and $h_i^{(w)}(t)$ represent the observed longitudinal eGFR measurements and the hazard functions for the j-th recurrent and w-th competing-risk terminal events for the i-th subject, respectively. Note that different time indices are utilized across the submodels in (1). The longitudinal and competing-risk terminal submodels are parameterized using follow-up time indexed by t, whereas the recurrent event submodel employs gap time, indexed by g_{ij}, which refers to the time interval between the $(j-1)$-th and j-th recurrent events for the i-th subject.

For clarity, we separate the covariates into two groups: primary covariates (primary risk factors) and secondary covariates (secondary risk factors). The primary covariates, denoted by $\mathbf{Z}_i = (Z_{i1}, \ldots, Z_{id})^\top$, are the main risk factors of interest. In our data application, these include diabetes, hypertension and history of CVD, which are key contributors to morbidity and mortality in CKD patients. The recurrent event submodel captures how these primary risk factors influence the occurrence of the first, second, and subsequent CV events, with these effects modeled through event-varying coefficients $\boldsymbol{\phi}_{rj}$. The secondary risk factors, denoted by $\mathbf{X}_i = (X_{i1}, \ldots, X_{id'})^\top$, comprise a broader set of covariates, including demographic variables, comorbidities and laboratory measurements. These covariates account for additional variability and allow for a more comprehensive characterization of the patient population. The regression coefficients for these secondary and primary covariates are denoted by $\boldsymbol{\beta} = (\boldsymbol{\beta}_\ell^\top, \boldsymbol{\beta}_r^\top, \boldsymbol{\beta}_t^{(1)\top}, \boldsymbol{\beta}_t^{(2)\top})$ and $\boldsymbol{\phi} = (\boldsymbol{\phi}_\ell^\top, \boldsymbol{\phi}_r^\top, \boldsymbol{\phi}_t^{(1)\top}, \boldsymbol{\phi}_t^{(2)\top})$, respectively, where $\boldsymbol{\phi}_r = (\boldsymbol{\phi}_{r1}^\top, \ldots, \boldsymbol{\phi}_{rJ_{\max}}^\top)^\top$ denotes the event-varying coefficient vector of the recurrent event submodel, and $J_{\max}$ denotes the maximum number of recurrent events among all subjects, i.e., $J_{\max} = \max(J_1, \ldots, J_n)$. Note that although all the submodels in (1) include a common set of covariates, the proposed joint model can easily be extended to accommodate design vectors with different dimensionality and composition for each submodel separately.

In the proposed recurrent event submodel, the recurrent event effect is modeled not only via $\boldsymbol{\phi}_{rj}$, the event-varying effect of covariates, but also via α_m, the additional risk introduced by the mth event (with $m = 1, \ldots, J_{\max} - 1$, and $\alpha_0 = 0$), where $\boldsymbol{\alpha} = (\alpha_1, \ldots, \alpha_{J_{\max}-1})$ denotes the event effect vector. Hence, $\exp(\alpha_m)$ is the hazard ratio of having an event (e.g., next CV event) for a patient with m previous events relative to a patient with $(m-1)$ previous events.

The interdependency among the submodels within the proposed joint model is established through shared random effects and the true underlying values of longitudinal biomarker, $\xi_i(t)$. Specifically, the dependency between the longitudinal and recurrent outcomes is captured via random effects: the random intercept b_{i0} and random slope b_{i1}, denoted as $\mathbf{b}_i = (b_{i0}, b_{i1})^\top$, and their association is quantified by the regression parameters η_{r0} and η_{r1}. Additionally, a frailty term, ν_i, is incorporated into the model to account for unobserved subject-specific heterogeneity that is not explained by the covariates or the longitudinal process $\xi_i(t)$, as well as the dependency among recurrent events. This frailty term also links the recurrent outcomes to competing risks, with the strength of this association described by the parameter $\zeta^{(w)}$. Further-

more, each competing risk w is assumed to depend on the true but unobserved values of the longitudinal biomarker, $\xi_i(t)$, which serves as a crucial link between the longitudinal and the w-th competing-risk terminal processes. This dependency is captured through the regression parameter $\eta_t^{(w)}$, which enables direct interpretation of the biomarker's predictive impact on each competing risk and allows comparisons of its effects across different competing risks. In addition, in the proposed BM-JM, the entire longitudinal measurement profile up to the prediction time t is integrated into the competing-risk terminal submodels, alongside the frailty term ν_i from the recurrent event submodel. This framework facilitates flexible and dynamic survival probability predictions for competing-risk terminal outcomes. Notably, ν_i and $\xi_i(t)$ serve distinct purposes in the joint modeling. The frailty term ν_i captures unobserved subject-specific heterogeneity and the dependency among recurrent events. Additionally, ν_i acts as a bridge linking the recurrent events to competing-risk hazards. In contrast, $\xi_i(t)$ represents the true underlying values of the longitudinal biomarker and directly associate the longitudinal outcomes with the competing-risk hazards. By modeling ν_i and $\xi_i(t)$ separately, the proposed framework achieves clearer interpretability of their respective roles and contributions to the joint model.

The vector of combined random effects is denoted by $\mathbf{u}_i = (\mathbf{b}_i^\mathsf{T}, \nu_i)^\mathsf{T}$ where $\mathbf{b}_i^\mathsf{T}$ and ν_i are assumed to be independent, and $\mathbf{u}_i$ follows a multivariate normal distribution $\mathbf{u}_i \sim N(\mathbf{0}, \mathbf{\Sigma})$ with $\mathbf{\Sigma} = \left[\mathbf{\Sigma}_b\ \mathbf{0}; \mathbf{0}\ \sigma_\nu^2\right]$, $\mathbf{\Sigma}_b = \left[\sigma_{b_0}^2\ \sigma_{01}; \sigma_{01}\ \sigma_{b_1}^2\right]$, $\sigma_{01} = \rho_b \sigma_{b_0} \sigma_{b_1}$, and ρ_b denoting the correlation between the random intercept and slope terms. In addition, $h_{r0}(g_{ij})$ denotes the baseline hazard function for the j-th recurrent process of the i-th subject, while $h_{t0}^{(w)}(t)$ represents the baseline hazard function for the wth competing-risk terminal process. The error term $\varepsilon_i(t)$ is assumed to be independent across time and follows a normal distribution $\varepsilon_i(t) \sim N(0, \sigma_\varepsilon^2)$. Furthermore, the error term is assumed to be mutually independent of the random effects. Finally, note that in our framework, longitudinal measurements and recurrent events can be observed at the same time; however, neither can be observed after the observed terminal event time T_i. This is consistent with the CRIC study, where eGFR measurements end at ESKD (not meaningful after ESKD) and obviously at death. Furthermore, a noninformative censoring mechanism is assumed for the terminal event, which ensures that the censoring mechanism for terminal events does not carry predictive information regarding the longitudinal process or the covariates.

2.2 Bayesian Estimation and Inference

To estimate the parameters of our joint model, we propose a Bayesian formulation and derive posterior inferences using a Markov Chain Monte Carlo (MCMC) algorithm. Let $\boldsymbol{\theta} = (\boldsymbol{\beta}, \boldsymbol{\phi}, \gamma, \boldsymbol{\alpha}, \boldsymbol{\eta}, \boldsymbol{\zeta}, \boldsymbol{\sigma}^2, \rho_b, \boldsymbol{\psi}_{h_0})^\mathsf{T}$ denote the vector of parameters from all submodels with $\boldsymbol{\beta} = (\boldsymbol{\beta}_\ell^\mathsf{T}, \boldsymbol{\beta}_r^\mathsf{T}, \boldsymbol{\beta}_t^{(1)\mathsf{T}}, \boldsymbol{\beta}_t^{(2)\mathsf{T}})$, $\boldsymbol{\phi} = (\boldsymbol{\phi}_\ell^\mathsf{T}, \boldsymbol{\phi}_r^\mathsf{T}, \boldsymbol{\phi}_t^{(1)\mathsf{T}}, \boldsymbol{\phi}_t^{(2)\mathsf{T}})$, $\boldsymbol{\alpha} = (\alpha_1, \ldots, \alpha_{J_{max}-1})$, $\boldsymbol{\eta} = (\eta_{r0}, \eta_{r1}, \eta_t^{(1)}, \eta_t^{(2)})$, $\boldsymbol{\zeta} = (\zeta^{(1)}, \zeta^{(2)})$, $\boldsymbol{\sigma}^2 = (\sigma_{b_0}^2, \sigma_{b_1}^2, \sigma_\varepsilon^2, \sigma_\nu^2)$, and $\boldsymbol{\psi}_{h_0}$ denoting the coefficients used to model the baseline hazard functions. The joint likelihood of the model is derived under the conditional independence assumption, that is, the random effects (REs: $\mathbf{u}_i = (\mathbf{b}_i^\mathsf{T}, \nu_i)^\mathsf{T}$) account for all dependencies among the multivariate outcomes, and that given the REs, the longitudinal, recurrent and competing-risk terminal processes are assumed to be independent. Conditional independence assumption leads to the conditional likelihood

$$
\begin{aligned}
p(\mathbf{Y}_i, \mathbf{G}_i, \boldsymbol{\lambda}_i, T_i, \delta_i \mid \mathbf{u}_i; \boldsymbol{\theta}) &= p(\mathbf{Y}_i \mid \mathbf{b}_i; \boldsymbol{\theta})\ p(\mathbf{G}_i, \boldsymbol{\lambda}_i \mid \mathbf{u}_i; \boldsymbol{\theta})\ p(T_i, \delta_i \mid \xi_i(\cdot), \nu_i; \boldsymbol{\theta}) \\
&= \prod_{k=1}^{K_i} p(Y_{ik} \mid \mathbf{b}_i; \boldsymbol{\theta})\ \prod_{j=1}^{J_i} p(G_{ij}, \lambda_{ij} \mid \mathbf{u}_i; \boldsymbol{\theta})\ p(T_i, \delta_i \mid \xi_i(\cdot), \nu_i; \boldsymbol{\theta}),
\end{aligned}
$$

where for the ith patient, $\mathbf{Y}_i = (Y_{i1}, \ldots, Y_{iK_i})^\top$ denotes the $K_i \times 1$ vector of longitudinal outcomes with $Y_{ik} = Y_i(t_{ik})$, $k = 1, \ldots, K_i$, and $\mathbf{G}_i = (G_{i1}, \ldots, G_{iJ_i})^\top$ and $\boldsymbol{\lambda}_i = (\lambda_{i1}, \ldots, \lambda_{iJ_i})^\top$ are the $J_i \times 1$ vectors of recurrent event times and recurrent event indicators, respectively. Hence, the posterior distribution is given by

$$\begin{aligned} p(\boldsymbol{\theta}, \mathbf{u}_i \mid \mathbf{Y}_i, \mathbf{G}_i, \boldsymbol{\lambda}_i, T_i, \delta_i) &\propto p(\mathbf{Y}_i, \mathbf{G}_i, \boldsymbol{\lambda}_i, T_i, \delta_i \mid \mathbf{u}_i, \boldsymbol{\theta})\ p(\mathbf{u}_i, \boldsymbol{\theta}) \\ &\propto p(\mathbf{Y}_i \mid \mathbf{b}_i; \boldsymbol{\theta})\ p(\mathbf{G}_i, \boldsymbol{\lambda}_i \mid \mathbf{u}_i; \boldsymbol{\theta})\ p(T_i, \delta_i \mid \xi_i(\cdot), \nu_i; \boldsymbol{\theta})\ p(\mathbf{u}_i \mid \boldsymbol{\theta})\ p(\boldsymbol{\theta}). \end{aligned}$$

In our data application, where the longitudinal outcome is continuous, the likelihood contributions from each submodel is given by

$$p(\mathbf{Y}_i \mid \mathbf{b}_i, \boldsymbol{\theta}) = \prod_{k=1}^{K_i} \frac{1}{\sqrt{2\pi\sigma_\varepsilon^2}} \exp\left[\frac{\{Y_{ik} - (\mathbf{X}_i^\top \boldsymbol{\beta}_\ell + \mathbf{Z}_i^\top \boldsymbol{\phi}_\ell + \gamma t_{ik} + b_{i0} + b_{i1} t_{ik})\}^2}{2\sigma_\varepsilon^2}\right],$$

$$\begin{aligned} p(\mathbf{G}_i, \boldsymbol{\lambda}_i \mid \mathbf{u}_i, \boldsymbol{\theta}) = \prod_{j=1}^{J_i} \Bigg[&\left\{ h_{r0}(G_{ij}) \exp\left(\mathbf{X}_i^\top \boldsymbol{\beta}_r + \mathbf{Z}_i^\top \boldsymbol{\phi}_{rj} + \sum_{m=0}^{j-1} \alpha_m + \eta_{r0} b_{i0} + \eta_{r1} b_{i1} + \nu_i \right) \right\}^{\lambda_{ij}} \\ &\times \exp\left\{ - \int_0^{G_{ij}} h_{r0}(g) \exp\left(\mathbf{X}_i^\top \boldsymbol{\beta}_r + \mathbf{Z}_i^\top \boldsymbol{\phi}_{rj} + \sum_{m=0}^{j-1} \alpha_m + \eta_{r0} b_{i0} + \eta_{r1} b_{i1} + \nu_i \right) \mathrm{d}g \right\} \Bigg], \end{aligned} \tag{2}$$

and

$$\begin{aligned} p(T_i, \delta_i \mid \xi_i(\cdot), \nu_i, \boldsymbol{\theta}) = \prod_{w=1}^{2} \Bigg[&\left\{ h_{t0}^{(w)}(T_i) \exp\left(\mathbf{X}_i^\top \boldsymbol{\beta}_t^{(w)} + \mathbf{Z}_i^\top \boldsymbol{\phi}_t^{(w)} + \eta_t^{(w)} \xi_i(T_i) + \zeta^{(w)} \nu_i \right) \right\}^{I(\delta_i = w)} \\ &\times \exp\left\{ - \int_0^{T_i} h_{t0}^{(w)}(v) \exp\left(\mathbf{X}_i^\top \boldsymbol{\beta}_t^{(w)} + \mathbf{Z}_i^\top \boldsymbol{\phi}_t^{(w)} + \eta_t^{(w)} \xi_i(v) + \zeta^{(w)} \nu_i \right) \mathrm{d}v \right\} \Bigg], \end{aligned} \tag{3}$$

where $\xi_i(t) = \mathbf{X}_i^\top \boldsymbol{\beta}_\ell + \mathbf{Z}_i^\top \boldsymbol{\phi}_\ell + \gamma t + b_{i0} + b_{i1} t$ denotes the value of the true but unobserved biomarker for subject i at time point t. Note that the integrals in (2) and (3) do not have closed-form solutions and the 15-point Gauss-Kronrod quadrature rule (Kahaner et al., 1989) is employed to approximate the integrals.

Bayesian P-splines with a relatively large number of equally spaced knots are employed in estimation of the baseline hazard functions. To avoid overfitting, a roughness penalty is incorporated as proposed by Eilers and Marx (1996). Specifically, let $h_0(t)$ denote any baseline hazard function in the recurrent or competing-risk event submodels. It is targeted via $\log\{h_0(t)\} = \sum_{q=1}^{Q} \psi_{h_0,q} B_q(t)$, where $B_q(t)$ denotes the B-spline basis functions and $\boldsymbol{\psi}_{h_0} = \{\psi_{h_0,1}, \ldots, \psi_{h_0,Q}\}^\top$ denotes the corresponding Q-dimensional vector of spline coefficients. Note that while we use Bayesian P-splines with equal number of knots in the estimation of all baseline hazard functions in our data application, our proposed estimation and inference procedure can accommodate both parametric and other nonparametric forms for baseline hazard functions, and allow for the adoption of varying numbers of knots within each baseline hazard function across different submodels.

The priors for fixed-effects parameters $\boldsymbol{\beta} = (\boldsymbol{\beta}_\ell^\top, \boldsymbol{\beta}_r^\top, \boldsymbol{\beta}_t^{(1)\top}, \boldsymbol{\beta}_t^{(2)\top})$, $\boldsymbol{\phi} = (\boldsymbol{\phi}_\ell^\top, \boldsymbol{\phi}_r^\top, \boldsymbol{\phi}_t^{(1)\top}, \boldsymbol{\phi}_t^{(2)\top})$, γ, and $\boldsymbol{\alpha} = (\alpha_1, \ldots, \alpha_{J_{\max}-1})$, and the association parameters $\boldsymbol{\eta} = (\eta_{r0}, \eta_{r1}, \eta_t^{(1)}, \eta_t^{(2)})$ and $\boldsymbol{\zeta} = (\zeta^{(1)}, \zeta^{(2)})$, are taken to be normal with mean zero and variance $\sigma_\star^2$, where the hyperparameters are set as inverse gamma (IG): $\sigma_\star^2 \sim \mathrm{IG}(a_{1\star}, a_{2\star})$. IG priors are also assumed for the variance terms $\boldsymbol{\sigma}^2 = (\sigma_{b_0}^2, \sigma_{b_1}^2, \sigma_\varepsilon^2, \sigma_\nu^2)$, i.e., $\sigma_*^2 \sim \mathrm{IG}(a_{1*}, a_{2*})$ ($*$ denoting b_0, b_1, ε or ν), and a uniform prior

is assumed for ρ_b, the correlation between the random intercept and slope terms $\mathbf{b}_i = (b_{i0}, b_{i1})^\mathsf{T}$. Note that we assign the same IG prior for the variance terms in $\boldsymbol{\sigma}^2$, however, our method can accommodate different priors for each variance term if needed. In the estimation of the baseline hazard functions, normal priors are used for the spline coefficients, such that $\boldsymbol{\psi}_{h_0}|\kappa_{h_0} \sim N(0, \kappa_{h_0}\mathcal{P}_{h_0})$, where κ_{h_0} denotes the variance parameter controlling the smoothness of the baseline hazard functions, and $\mathcal{P}_{h_0}$ denotes the penalty matrix. Similar to the variance terms, IG priors are used for the variance parameter κ_{h_0}, $\kappa_{h_0} \sim \text{IG}(a_{1\kappa}, a_{2\kappa})$, where $a_{1\kappa}$ is set to 1 and $a_{2\kappa}$ to a small number, following Jullion and Lambert (2007). The penalty matrix $\mathcal{P}_{h_0}$ is computed using the second-order difference matrix Ω of dimension $Q \times Q$ in our applications, i.e., $\mathcal{P}_{h_0} = \Omega^\mathsf{T}\Omega + 10^{-4}I$, with I representing the $Q \times Q$ identity matrix. The addition of a small positive constant (10^{-4}) to the diagonal elements of the product $\Omega^\mathsf{T}\Omega$ helps stabilize the computation and prevents issues related to singularity or numerical instability (Eilers and Marx, 1996). Specific values for these priors are detailed in Appendix A of the online Supplementary Materials. Finally, pointwise credible intervals (CIs) are utilized for inference based on the posterior sample. Let τ denote a parameter within the full parameter vector $\boldsymbol{\theta} = (\boldsymbol{\beta}, \boldsymbol{\phi}, \gamma, \boldsymbol{\alpha}, \boldsymbol{\eta}, \boldsymbol{\zeta}, \boldsymbol{\sigma}, \rho_b, \boldsymbol{\psi}_{h_0})^\mathsf{T}$, and $\widehat{\tau}$ and $\text{SD}(\tau)$ denote the mean and standard deviation of τ obtained based on the MCMC samples, respectively. Then the $(1-\alpha)$ pointwise credible intervals are given by $\left[\widehat{\tau} \pm \Phi_{\alpha/2}\text{SD}(\tau)\right]$, where $\Phi_{\alpha/2}$ denotes the $100 \times (1-\alpha/2)$-percentile of the standard normal distribution.

3 Dynamic Prediction of Cumulative Incidence Functions

3.1 Proposed Prediction Algorithm

For a BM-JM fit using a training dataset $\mathcal{D}_n = \{\mathbf{Y}_i, \mathbf{G}_i, \boldsymbol{\lambda}_i, T_i, \delta_i; i = 1, \ldots, n\}$ with n subjects, we consider predicting survival probabilities for each competing-risk terminal outcome on an independent testing dataset of n_p subjects. More specifically, the cumulative incidence probability of each competing-risk terminal outcome is targeted for a new patient p ($p = 1, \ldots, n_p$) with baseline characteristics, a set of longitudinal measurements $\mathcal{Y}_p(t) = \{Y_p(t_{pk}) : 0 < t_{pk} \leqslant t,\ k = 1, \ldots, K\}$ and recurrent events history $\mathcal{R}_p(t) = \{\{G_{pj}, \lambda_{pj}\} : 0 < \sum_{j=1}^{J} G_{pj} \leqslant t, j = 1, \ldots, J\}$ till the prediction time t. Given that patient p has not experienced a competing-risk terminal event up to time t, the goal is to predict the subject-p-specific cumulative incidence probability for patient p to experience the wth competing-risk terminal event within the time interval $(t, s]$ given all information available till time t,

$$\pi_p^{(w)}(t, s) \quad = \quad P\left(t < T_p^{*(w)} < s \mid \cup_{w=1}^{2}(T_p^{*(w)} > t), \mathcal{Y}_p(t), \mathcal{R}_p(t), \mathcal{D}_n\right),$$

where $s = t + \Delta t$ with $\Delta t > 0$ denoting the prediction window. In this definition, we assume that the previous longitudinal measurements, as well as recurrent events are directly related to the competing-risk failure mechanism.

Note that these predictions are dynamic in the sense that they change with increasing prediction time t and available individual longitudinal and recurrent events information. Under the Bayesian formulation of the joint model, the estimation of $\pi_p^{(w)}(t, s)$ is based on the corresponding posterior predictive distributions, namely,

$$\pi_p^{(w)}(t, s) \quad = \quad \int P\left(t < T_p^{*(w)} < s \mid \cup_{w=1}^{2}(T_p^{*(w)} > t), \mathcal{Y}_p(t), \mathcal{R}_p(t); \boldsymbol{\theta}\right) \times p(\boldsymbol{\theta} \mid \mathcal{D}_n)\mathrm{d}\boldsymbol{\theta}. \qquad (4)$$

The second term of the integrand in (4), $p(\boldsymbol{\theta} \mid \mathcal{D}_n)$, is the posterior distribution of the parameters

given the observed data $\mathcal{D}_n$. The first term of the integrand in (4) can be given as

$$\begin{aligned} &\int P\left(t < T_p^{*(w)} < s \mid \cup_{w=1}^{2}(T_p^{*(w)} > t), \mathcal{Y}_p(t), \mathcal{R}_p(t), \mathbf{u}_p; \boldsymbol{\theta}\right) \\ \times \quad & p\left(\mathbf{u}_p \mid \cup_{w=1}^{2}(T_p^{*(w)} > t), \mathcal{Y}_p(t), \mathcal{R}_p(t); \boldsymbol{\theta}\right) \mathrm{d}\mathbf{u}_p. \end{aligned} \tag{5}$$

Using the full conditional independence assumptions, that is, the random effects $\mathbf{u}_p$ account for all dependencies among the multivariate outcomes, (5) can further be simplified as

$$\int P\left(t < T_p^{*(w)} < s \mid \cup_{w=1}^{2}(T_p^{*(w)} > t), \mathbf{u}_p; \boldsymbol{\theta}\right) \quad p\left(\mathbf{u}_p \mid \cup_{w=1}^{2}(T_p^{*(w)} > t), \mathcal{Y}_p(t), \mathcal{R}_p(t); \boldsymbol{\theta}\right) \mathrm{d}\mathbf{u}_p.$$

Furthermore, by the definition of conditional probability, (5) can be expressed as

$$\begin{aligned} &\int \frac{P\left(t < T_p^{*(w)} < s, \cup_{w=1}^{2}(T_p^{*(w)} > t) \mid \mathbf{u}_p; \boldsymbol{\theta}\right)}{P\left(\cup_{w=1}^{2}(T_p^{*(w)} > t) \mid \mathbf{u}_p; \boldsymbol{\theta}\right)} \quad p\left(\mathbf{u}_p \mid \cup_{w=1}^{2}(T_p^{*(w)} > t), \mathcal{Y}_p(t), \mathcal{R}_p(t); \boldsymbol{\theta}\right) \mathrm{d}\mathbf{u}_p \\ \equiv \quad &\int \frac{\mathrm{CIF}_p^{(w)}(t, s)}{\mathrm{S}_p(t)} \times p\left(\mathbf{u}_p \mid \cup_{w=1}^{2}(T_p^{*(w)} > t), \mathcal{Y}_p(t), \mathcal{R}_p(t); \boldsymbol{\theta}\right) \mathrm{d}\mathbf{u}_p, \end{aligned} \tag{6}$$

where

$$\begin{aligned} \mathrm{S}_p(t) &= \prod_{w=1}^{2}\left[\exp\left\{-\int_0^t h_{t0}^{(w)}(v)\exp\left(\mathbf{X}_p^{\top}\boldsymbol{\beta}_t^{(w)} + \mathbf{Z}_p^{\top}\boldsymbol{\phi}_t^{(w)} + \eta_t^{(w)}\xi_p(v) + \zeta^{(w)}\nu_p\right)\mathrm{d}v\right\}\right] \text{ and} \\ \mathrm{CIF}_p^{(w)}(t, s) &= \int_t^s h_{t0}^{(w)}(v)\exp\left(\mathbf{X}_p^{\top}\boldsymbol{\beta}_t^{(w)} + \mathbf{Z}_p^{\top}\boldsymbol{\phi}_t^{(w)} + \eta_t^{(w)}\xi_p(v) + \zeta^{(w)}\nu_p\right)\mathrm{S}_p(v)\mathrm{d}v \end{aligned} \tag{7}$$

denote the subject-p-specific overall survival function across two competing-risk outcomes (i.e., the conditional probability that subject p has experienced neither of the competing terminal events till time t) and the cumulative incidence function for the wth competing-risk terminal event (i.e., the conditional probability that subject p experiences the wth competing-risk terminal event within the time interval $(t, s]$), respectively. Thus, the first component of the integrand in $\pi_p^{(w)}(t, s)$ can be addressed using (6), while the second component is estimated based on the posterior distribution of the model parameters from the training dataset $\mathcal{D}_n$. A Monte Carlo estimate of $\pi_p^{(w)}(t, s)$ is obtained through a simulation scheme. The detailed algorithm for this process is provided in Appendix B, with a summarized procedure outlined in Table S1 of the Supplementary Materials.

3.2 Predictive Accuracy Measures

To assess the predictive accuracy of the proposed BM-JM, we used two widely recognized metrics: the area under the receiver operating characteristic curve (AUC) and the expected Brier score (BS). AUC captures the model's overall ability to distinguish between different outcomes, while BS measures the average discrepancy between predicted risks and observed event probabilities. Given the dynamic nature of predictions in a competing risks framework, we utilized an adapted version of these measures to evaluate the BM-JM's performance across varying prediction time windows. To handle right-censored data, as seen in our CRIC study, we applied the Inverse Probability of Censoring Weighting (IPCW) method to estimate the dynamic AUC

and BS, denoted as $\widehat{\text{AUC}}^{(w)}(t, s)$ and $\widehat{\text{BS}}^{(w)}(t, s)$ for the w-th competing risk. This approach accounts for censored observations, ensuring reliable performance evaluation. Detailed definitions, derivations, and implementation of these dynamic AUC and BS in a competing risks context, along with their computation under the BM-JM framework, are presented in Appendix C of the Supplementary Materials.

R codes and documentation for fitting BM-JM and predicting dynamically updated survival probabilities for future subjects, as well as predictive accuracy measures, are made publicly available at https://github.com/dsenturk/BM-JM. Due to the absence of closed-form solutions for the posterior distributions, the proposed model was fitted using the Bayesian software JAGS (version 4.3.0) via the `rjags` package (with more details deferred to Appendix A of the Supplementary Materials).

4 Application to the CRIC Study

4.1 Study Cohort

The CRIC study, initiated by NIDDK in 2001, is an ongoing multicenter prospective longitudinal cohort study that enrolls adults with mild to moderate CKD. After exclusion of patients with missing laboratory data (7.4%) and with CV hospital admission and death dates within one-day apart (0.2%), the final analysis cohort included 5,194 patients. Comprehensive baseline characteristics and pertinent risk factors of the analysis cohort are summarized in Table S2 (of the Supplementary Materials). As outlined in Section 2.1, our approach segregates covariates considered into primary ($\mathbf{Z}_i$) and secondary ($\mathbf{X}_i$) risk factors. Primary risk factors include diabetes, hypertension, and history of CVD. Secondary risk factors include demographic variables (age, sex, race), behavioral factors (current smoker, body mass index (BMI)), cardiovascular parameters (systolic and diastolic blood pressure (SBP/DBP), high blood pressure (blood pressure (BP) > 130/80 mmHg), angle-brachial index (ABI)), laboratory measures (hemoglobin A1c (HbA1c), calcium, creatinine (Roche adjusted), glucose), and use of angiotensin-converting enzyme inhibitor (ACEI) or angiotensin receptor blocker (ARB) therapy. Within the analysis cohort, age of patients ranged between 21 and 79 years (mean 59.6, standard deviation (SD) 10.7), where 43.4% of patients were females. Approximately 12.5% of patients were current smokers. In addition, 51.1%, 86.5%, and 27.7% of patients had a history of diabetes, hypertension, and CVD, respectively. The median follow-up duration extended to 11.8 years, with a maximum follow-up period of approximately 16.9 years. Three fourths of the analysis cohort had survived beyond five years.

Our analysis focused on the interdependent outcomes of longitudinal eGFR progression, recurrent hospitalizations due to CV events, and competing-risk terminal events defined as kidney failure and death in the CKD population. The mean baseline eGFR was at 48.4 ml/min/1.73m^2 (SD 15.6, median 48.2, first-third quartile (Q1-Q3) 37.1–58.8). The longitudinal eGFR trajectories of 200 randomly selected patients, given in Figure 1 (A), illustrate the heterogeneity in kidney function in the analysis cohort throughout follow-up. CV events considered included congestive heart failure, myocardial infarction, cerebrovascular accident, peripheral arterial disease and atrial fibrillation. In the recurrent event submodel, we focus on the first three hospitalizations due to CV events, typically of most clinical relevance. Within the analysis cohort, among the 1,582 subjects with one or more CV events, about 80% of patients experienced 1 (787), 2 (311), or 3 (161) CV events. The event rates for the two competing terminal events, ESKD and death, were comparable, at 25.53% and 20.91%, respectively. Figure 1 (B) shows the cumu-

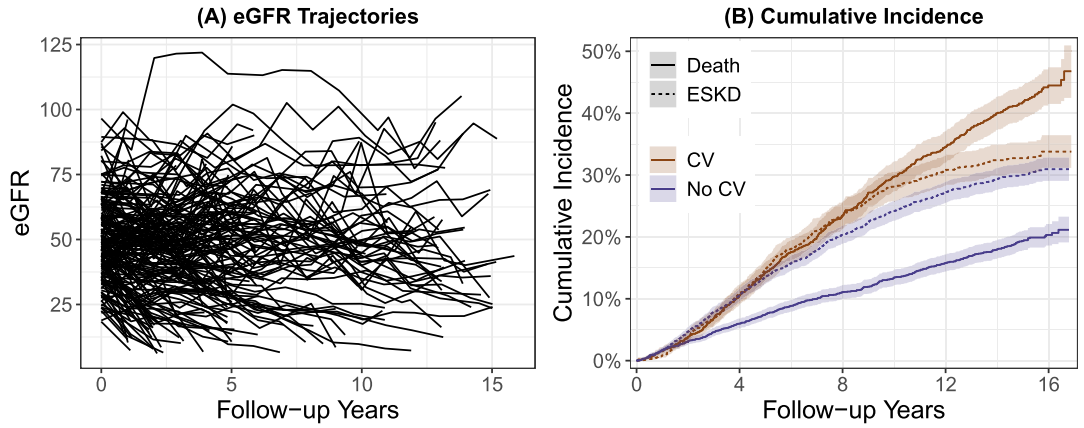

Figure 1: (A) longitudinal estimated glomerular filtration rate (eGFR) for 200 randomly selected individuals, and (B) cumulative incidence curves for ESKD and death from the analysis cohort patients with/out CV events.

lative incidence of these events among CKD patients, stratified by the presence or absence of CV events. Notably, patients with CV events were more likely to progress to death, while those without CV events had a higher probability of progressing to ESKD. Furthermore, the progression to ESKD occurred at similar rates regardless of CV event status. However, the likelihood of death was significantly higher among CKD patients who experienced CV events, emphasizing the strong association between recurrent CV events and the risk of mortality.

4.2 Risk Factors and Interrelationships Among Outcomes

The proposed BM-JM modeling framework was applied to the CRIC analysis cohort. To evaluate the predictive accuracy of the proposed dynamic prediction procedure, an independent testing dataset of size $n_p = 50$ was randomly selected from the analysis cohort and excluded from the model fitting process. Results from the BM-JM are presented in Table 1 and Table S3 (of the Supplementary Materials). Additional details on model fitting, including the specific choices of tuning and hyperparameters, the number of burn-in iterations, and the detailed prior distributions for model parameters, are provided in Appendix A of the Supplementary Materials.

As outlined in Table 1(A), the longitudinal eGFR exhibited a yearly decline of -1.51 ml/min/1.73m^2 (95% credible interval (CI): -1.59 to -1.42) per year. Two primary risk factors were significantly associated with lower eGFR: hypertension (-1.59, CI: -2.26 to -0.93) and a history of CVD (-0.57, CI: -1.01 to -0.13). Additional factors associated with lower eGFR included being female (-9.96), ACEI/ARB therapy (-1.18), high BP (-0.55), older age (-0.30), and higher levels of creatinine (-25.50), HbA1c (-0.24) and SBP (-0.03). Conversely, factors associated with higher eGFR included being black (6.32), belonging to a race other than white or black (0.87), and higher levels of calcium (1.01), hemoglobin (0.16), and glucose (0.01). Notably, diabetes, the third primary risk factor, was not found to be significantly associated with eGFR after adjusting for relevant laboratory markers (e.g., HbA1c). Insights from Table S3(B) further reveal that subject-specific variation accounted for a substantial proportion of total variation in eGFR. Additionally, a positive correlation ($\rho_b = 0.31$) was observed between the random effects for the intercept and slope.

Table 1: Results from the proposed BM-JM of (A) longitudinal estimated glomerular filtration rate (eGFR), (B) recurrent cardiovascular (CV) events, (C1 and C2) competing-risk terminal events (i.e., (C1) for ESKD and (C2) for death). Effect sizes (estimates and hazard ratios (HRs)) are given for one unit change in covariates.

	(A) Longitudinal eGFR	**(B) Recurrent CV Events**	**(C1) Terminal ESKD Event**	**(C2) Terminal Death Event**
Variable	Estimate (95% CI)	HR (95% CI)	HR (95% CI)	HR (95% CI)
Intercept	52.085 (51.323, 52.834)*	–	–	–
Time, γ	−1.505 (−1.592, −1.418)*	–	–	–
Age (years)	−0.304 (−0.327, −0.282)*	1.035 (1.028, 1.041)*	0.965 (0.957, 0.971)*	1.078 (1.060, 1.101)*
Non-Hispanic Black*	6.320 (5.836, 6.769)*	0.902 (0.807, 1.008)	1.313 (1.103, 1.564)*	0.930 (0.716, 1.197)
Other*	0.870 (0.233, 1.492)*	0.840 (0.715, 0.980)*	1.127 (0.923, 1.385)	1.037 (0.730, 1.484)
Female	−9.961 (−10.404, −9.497)*	0.890 (0.795, 0.998)*	0.454 (0.381, 0.544)*	0.478 (0.348, 0.633)*
Smoker	−0.423 (−1.093, 0.279)	1.391 (1.201, 1.611)*	1.188 (0.973, 1.441)	2.995 (2.100, 4.486)*
Body Mass Index	0.018 (−0.012, 0.048)	1.016 (1.009, 1.023)*	0.993 (0.983, 1.003)	1.016 (1.002, 1.031)*
ABI < 0.9	−0.135 (−0.729, 0.450)	1.371 (1.214, 1.550)*	1.089 (0.903, 1.309)	2.226 (1.644, 3.077)*
ACEI/ARB use	−1.179 (−1.686, −0.709)*	0.948 (0.845, 1.066)	1.047 (0.891, 1.229)	0.796 (0.608, 1.023)
Glucose (mg/dL)	0.007 (0.001, 0.012)*	1.000 (0.999, 1.002)	1.000 (0.998, 1.001)	0.999 (0.996, 1.002)
Hemoglobin A1c (%)	−0.237 (−0.439, −0.041)*	1.125 (1.078, 1.176)*	1.073 (1.013, 1.134)*	1.266 (1.137, 1.426)*
Hemoglobin (g/dL)	0.164 (0.029, 0.296)*	0.952 (0.920, 0.985)*	0.922 (0.880, 0.968)*	0.858 (0.791, 0.924)*
Calcium (mg/dL)	1.014 (0.577, 1.464)*	0.828 (0.746, 0.919)*	0.791 (0.685, 0.914)*	0.925 (0.736, 1.161)
Creatinine (mg/dL)	−25.497 (−25.941, −25.048)*	1.416 (1.274, 1.575)*	0.499 (0.419, 0.589)*	1.305 (0.954, 1.815)
High BP	−0.547 (−1.124, −0.028)*	0.997 (0.865, 1.156)	1.001 (0.810, 1.235)	0.857 (0.611, 1.198)
SBP (mmHg)	−0.032 (−0.049, −0.017)*	1.003 (1.000, 1.007)	1.005 (1.000, 1.010)	1.014 (1.005, 1.022)*
DPB (mmHg)	0.012 (−0.011, 0.032)	0.997 (0.992, 1.002)	0.999 (0.992, 1.006)	0.997 (0.985, 1.009)
Diabetes	−0.087 (−0.582, 0.408)	–	1.226 (1.014, 1.481)*	1.255 (0.939, 1.679)
Diabetes - ϕ_{11}	–	1.158 (1.003, 1.336)*	–	–
Diabetes - ϕ_{12}	–	0.961 (0.799, 1.162)	–	–
Diabetes - ϕ_{13}	–	0.787 (0.634, 1.018)	–	–
Hypertension	−1.588 (−2.262, −0.928)*	–	1.230 (0.945, 1.623)	1.380 (0.960, 1.998)
Hypertension - ϕ_{21}	–	1.618 (1.311, 2.042)*	–	–
Hypertension - ϕ_{22}	–	1.149 (0.838, 1.600)	–	–
Hypertension - ϕ_{23}	–	1.309 (0.874, 2.014)	–	–
CVD	−0.566 (−1.006, −0.126)*	–	1.290 (1.097, 1.510)*	3.065 (2.331, 4.233)*
CVD - ϕ_{31}	–	2.654 (2.349, 3.001)*	–	–
CVD - ϕ_{32}	–	1.718 (1.445, 2.028)*	–	–
CVD - ϕ_{33}	–	1.632 (1.315, 2.028)*	–	–
α_1	–	5.755 (3.885, 8.390)*	–	–
α_2	–	1.567 (0.926, 2.656)	–	–

1. $*$ 95% credible interval (CI) does not include estimate of 0 or hazard ratio (HR) of 1;
2. $\star$ Reference group: Non-Hispanic White;
3. Angiotensin-converting enzyme inhibitor(ACEI); angiotensin receptor blocker (ARB); blood pressure (BP); cardiovascular disease (CVD); hemoglobin A1c (HbA1c); systolic and diastolic BP (SBP, DBP)

Next, we explored the risk factors associated with recurrent CV events, as outlined in Table 1(B). Among the secondary risk factors, being a smoker (hazard ratio (HR) 1.39), having an ABI < 0.9 (HR 1.37), older age (HR 1.04), and higher levels of BMI (HR 1.02), HbA1c (HR 1.13), and creatinine (HR 1.42) were significantly associated with an increased hazard of recurrent CV events. Conversely, belonging to a race other than white or black (HR 0.84), being female (HR 0.89), and having higher levels of hemoglobin (HR 0.95) and calcium (HR 0.83) were associated with a decreased hazard of CV events. The event-varying effects of primary risk factors on the 1st, 2nd and 3rd CV events, as well as the event effects (i.e., the effect of prior CV events on future CV events), were also studied. As shown in Table 1(B), patients with a history of CVD had the highest HR for the first CV event (HR 2.65, CI: 2.35 to 3.00) compared to those without CVD. Although the hazard remained significantly elevated for the second (HR 1.72, CI: 1.45 to 2.03) and the third (HR 1.63, CI: 1.32 to 2.03) CV events, it was reduced by more than half compared to the risk for the first CV event. Patients with hypertension exhibited the second-highest HR for the first CV event (HR 1.62, CI: 1.31 to 2.04), while patients with diabetes showed only a 16% increased hazard for the first CV event (HR 1.16, CI: 1.00 to 1.34), potentially due to an indirect effect of diabetes mediated through HbA1c control. Notably, neither hypertension nor diabetes were significantly associated with subsequent CV events. Regarding the CV event effects ($\widehat{\alpha}$'s), the hazard of experiencing the next CV event for a CKD patient with one prior CV event was substantial compared to a patient with no prior events (HR 5.76, CI: 3.89 to 8.39). However, for a patient with two past CV events, the hazard of experiencing the next (third) CV event was drastically reduced and not statistically significant (HR 1.57, CI: 0.93 to 2.66).

For the risk factors influencing competing-risk terminal events (ESKD and death) (Tables 1(C1) and (C2)), a history of CVD was associated with higher hazards for both events, with a particularly elevated hazard for death (HR 3.07, CI: 2.33 to 4.23). Diabetes was associated with an increased hazard of ESKD only (HR 1.23, CI: 1.01 to 1.48), while hypertension was not significantly associated with either event. Elevated levels of HbA1c were linked to an increased hazard for both competing risks, whereas being female and having higher hemoglobin levels were associated with reduced hazard for both ESKD and death. Interestingly, age had opposing effects on the two competing risks, i.e., higher age was associated with a lower hazard for ESKD but a higher hazard for death. Additionally, some predictors had impacts only on one competing risk. For instance, being black (HR 1.31) was associated with a higher hazard of ESKD, while higher levels of hemoglobin (HR 0.92), calcium (HR 0.79) and creatinine (HR 0.50) were associated with reduced hazards of ESKD. In contrast, smoking (HR 3.00) and ABI < 0.9 (HR 2.23) were significantly associated with an increased hazard of death.

Regarding the interrelationships among multivariate outcomes (shown in Table S3(A)), individual variability explained by the random slope in longitudinal eGFR trajectories was significantly associated with recurrent CV events ($\eta_{r1} = -0.16$, CI: -0.19 to -0.13). This strong association aligns with expectations, as declining kidney function is well-documented to correlate with CV events in CKD patients (Go et al., 2004). In contrast, variability in the random intercept was not significantly associated with CV events ($\eta_{r0} = 0.004$, CI: -0.006 to 0.014). As highlighted in Section 1 and 2.1, a key innovation of the proposed BM-JM is its capacity to directly quantify associations between the longitudinal biomarker and competing-risk terminal events via $\eta_t^{(w)}$. Lower eGFR levels were strongly associated with ESKD ($\eta_t^{(1)} = -0.19$, CI: -0.20 to -0.18), while the direct effect of lower eGFR levels on death was much smaller ($\eta_t^{(2)} = -0.02$, CI: -0.03 to -0.01). This pattern is expected, as declining kidney function directly contributes to kidney failure, whereas the causes of death in CKD patients are more diverse and complex. Finally, recurrent CV events demonstrated a much stronger positive association with death

($\zeta^{(2)} = 2.82$, CI: 2.06 to 3.69) compared to their association with ESKD ($\zeta^{(1)} = 0.29$, CI: 0.07 to 0.51), which aligns with the higher probability of progression to death observed among CKD patients with CV events observed in Figure 1(B).

4.3 Comparison with Simpler Models

We compared the proposed BM-JM with other well-established models that overlook the joint outcomes structure. Specifically, our proposed BM-JM consists of three components: the longitudinal, recurrent and competing-risk terminal components. We decompose these components into three separate marginal models, each addressing a single outcome: the longitudinal model (L-M), the recurrent model (R-M) and the competing-risk terminal model (T-M). Additionally, we combine two of these components to form simplified joint models. Since one of our primary objectives is to make dynamic predictions for competing risks, we focus on two simplified joint models: (1) the joint model of longitudinal measurements and competing-risk terminal events (referred to as LT-JM), which excludes the recurrent component, and (2) the joint model of recurrent and competing-risk terminal events (referred to as RT-JM), which excludes the longitudinal component. All these models were applied to the CRIC study analysis cohort. Further details about these comparative models are provided in Appendix D of the Supplementary Materials, with results from three marginal models summarized in supplementary Table S4 (A-B-C) for the longitudinal eGFR (L-M), recurrent CV events (R-M), and competing-risk terminal events (T-M), respectively. Additionally, the results for the LT-JM and RT-JM fits are presented in supplementary Tables S5 and S6, respectively.

Comparison with marginal models: For the longitudinal eGFR, the results from the marginal model (L-M) (see Table S4(A)) were largely consistent with those of the proposed BM-JM. The effects of all covariates on eGFR trajectories, including their inference, were comparable between the two models. Notably, the primary covariates (diabetes, hypertension, and history of CVD) exhibited similar effects on eGFR across both models. However, the decline in kidney function over time was slightly attenuated in the marginal model (L-M -1.33 vs. BM-JM -1.51). For the recurrent CV events, while the overall conclusions for the primary covariates were similar between the marginal R-M (see Table S4(B)) and the BM-JM analyses, in terms of effect sizes and inference, some notable differences regarding the secondary covariates emerged. For instance, the effect of creatinine on recurrent CV events was smaller in the marginal R-M analysis (R-M HR 1.12 vs. BM-JM HR 1.42).

For the competing risks of ESKD and death, the marginal T-M analysis (see Table S4 (C1 and C2)) showed similar inference based on CIs for the primary covariates compared to the BM-JM. However, there were notable differences in effect estimates. For instance, the marginal T-M analysis yielded higher effect estimates for diabetes and history of CVD on ESKD but lower effect estimates for death compared to the BM-JM. Additionally, the T-M analysis estimated a stronger effect of smoking on ESKD (T-M HR 1.64 vs. BM-JM HR 1.19) but a weaker effect on death (T-M HR 1.80 vs. BM-JM HR 3.00). Notably, the marginal T-M analysis produced conflicting results for creatinine and female gender on ESKD compared to the BM-JM, i.e., the T-M estimated an HR of 11.82 for creatinine and 1.31 for female gender on ESKD, while the BM-JM estimated HRs of 0.50 and 0.45, respectively. Furthermore, while the effect of creatinine was statistically significant for death in the T-M analysis, it was not significant in the BM-JM.

Comparison with simpler joint models: For the LT-JM model fits (see supplementary Table S5), the results for the longitudinal eGFR and ESKD terminal submodels were generally

consistent with those obtained from the BM-JM. However, notable differences were observed in the death terminal submodel. Specifically, the effect estimates for being a smoker, having an ABI < 0.9, and a history of CVD on mortality were significantly attenuated in the LT-JM. This suggests that excluding the recurrent component impacts the death submodel's estimates, as expected, due to the stronger association of recurrent CV events with mortality.

In comparison, the differences between the RT-JM (see supplementary Table S6) and the BM-JM analyses were more pronounced. While the overall effects of covariates on recurrent CV events were similar across the two models, the estimates and inferences for the competing-risk components showed significant disparities. Except for the effect of a history of CVD on mortality, the effects of primary covariates on ESKD and death were markedly amplified in the RT-JM compared to the BM-JM. Substantial differences were particularly evident in the ESKD terminal submodel, which is more closely associated with longitudinal eGFR measurements than mortality. For instance, the RT-JM estimated an HR of 9.07 for creatinine and 1.21 for female gender, compared to HRs of 0.50 and 0.45, respectively, in the BM-JM. Additionally, the effect of creatinine on mortality was statistically significant in the RT-JM but not in the BM-JM. Regarding the correlation and covariance estimates, the variance for the frailty term ν_i and the correlation parameters $\zeta^{(w)}$ were significantly larger in the RT-JM. This is likely attributable to the omission of variability from the longitudinal component in each submodel of the RT-JM. As discussed in the next section, the changes in model fits using the LT-JM and RT-JM led to poorer dynamic prediction performance for both ESKD and death compared to the BM-JM. These performance gaps were particularly pronounced in the AUC and BS assessments for mortality predictions, where both simplified models demonstrated significantly lower accuracy.

4.4 Dynamic Prediction Results

Next, posterior samples from the BM-JM fit were used to estimate the cumulative incidence functions for ESKD and death, given a new patient's baseline characteristics, available eGFR measurements, and recurrent CV event profiles, as outlined in Section 3 and Table S1 (of the Supplementary Materials). Supplementary Figures S9 and S10 (C-J) present the median of 200 Monte Carlo realizations of $\pi_p^{(w)}(s,t)$, along with 95% pointwise CIs based on the percentiles of $\pi_p^{(w)}(s,t)$ over the Monte Carlo samples. These predictions are displayed for varying prediction times $t = 0, 2, 4, 6$ up to 14 years of follow-up for two patient pairs.

The first pair, Patients 23 and 24, shared nearly identical baseline characteristics: both were 58-year-old male CKD patients of other race with diabetes, hypertension, and a history of CVD at enrollment. Additionally, both experienced three recurrent CV events during follow-up (Figure S9(B)). However, their eGFR trajectories diverged significantly: Patient 23 maintained a relatively stable and higher eGFR profile throughout follow-up, whereas Patient 24 exhibited a steady decline in eGFR starting two years into follow-up (Figure S9(A)). These differences in eGFR trajectories had a profound impact on their predicted risks (as shown in Figure S9(C-J)). Patient 24 had a probability exceeding 0.6 of developing ESKD by year 6, which rose to over 0.8 by year 14, consistent with the observed outcome of being diagnosed with ESKD at 8.61 years. In contrast, Patient 23, despite having a slightly higher predicted mortality risk, displayed a much lower probability of developing ESKD, aligning with the observed outcome of death at 12.69 years. These results highlight the critical role of eGFR trajectories in predicting ESKD risk and demonstrate how incorporating longitudinal profiles can refine individualized risk predictions.

The second pair, Patients 12 and 10, also shared similar baseline characteristics: both were approximately 70-year-old male CKD patients of other race with diabetes, hypertension, and a history of CVD at baseline. Their eGFR trajectories during follow-up were roughly similar (see Figure S10(A)), with Patient 12 exhibiting a unique dip in eGFR values towards the end of follow-up, around 10 years. However, their recurrent CV event profiles differed significantly: Patient 12 experienced no recurrent CV events during follow-up, whereas Patient 10 underwent three successive CV events (Figure S10(B)). As shown in Figure S10(C-J), the ESKD risk predictions for these two patients were relatively similar, especially at $t = 6$ years. However, at earlier time points, when only baseline characteristics ($t = 0$) and eGFR trajectories up to two years ($t = 2$) were considered, Patient 12 exhibited a higher predicted risk of ESKD. In contrast, their mortality risk predictions diverged substantially: Patient 10's predicted mortality risk escalated to over 0.6 by year 14, whereas Patient 12's predicted mortality risk remained around 0.1. These predictions are consistent with the observed outcomes: Patient 12 progressed to ESKD towards the end of follow-up at year 10.77, while Patient 10 died at year 7.78, shortly after his last CV event. The inclusion of recurrent CV event data heavily influenced the differences in survival risk predictions for this pair. Additionally, the increased variability in predictions for Patient 10 at later years could be attributed to the reduced number of patients remaining in the study, leading to greater uncertainty in estimated hazards. This example, alongside the analysis of Patients 23 and 24, highlights the importance of integrating both longitudinal measurements and recurrent event data in prognostic modeling for CKD patients. Notably, these findings align with conclusions drawn from $\eta_t^{(w)}$ and $\zeta^{(w)}$, as well as observations in Figure 1(B), underscoring the strong correlation between longitudinal eGFR trajectories and ESKD, and between recurrent CV events and mortality.

To further evaluate the predictive accuracy of the dynamic prediction results obtained from the BM-JM and compare them with those from the comparative joint models, LT-JM and RT-JM, dynamic AUC and BS values were calculated using the testing dataset ($n_p = 50$) which was set aside from model fitting. The results (summarized in Figure S11) indicate that the overall prediction performance for ESKD surpasses that for mortality, as evidenced by higher AUC and lower BS values across all models in most time points. This finding aligns with expectations, as longitudinal eGFR trajectories are strong markers for kidney decline and progression to ESKD, whereas mortality in CKD patients is inherently more challenging to predict. For a fixed prediction time t, dynamic AUC values tend to decrease, and dynamic BS values tend to increase with a longer prediction time window Δt. This trend arises because even small differences between the true and estimated random effects are expected to translate to greater differences between the corresponding cumulative incidence functions as time progresses (i.e., for greater Δt). Notably, prediction accuracy does not necessarily improve as the prediction time t increases, despite the availability of additional longitudinal and recurrent data. This phenomenon reflects the interplay of two opposing factors: the accumulation of additional longitudinal and recurrent event information over time reduces the degree of shrinkage in the estimation of random effects. However, as the prediction time progresses, fewer patients remain in the study, leading to increased variability in the estimated hazard functions. These opposing forces may result in prediction accuracy remaining steady as t increases.

Importantly, the proposed BM-JM consistently outperforms both LT-JM and RT-JM, as evidenced by higher dynamic AUC and lower dynamic BS values for both ESKD and mortality risk predictions. This performance gap widens further as prediction time t increases, due to the increasing availability of recurrent/longitudinal data. While RT-JM, which incorporates recurrent CV events into the joint modeling, outperforms LT-JM, especially for mortality pre-

dictions at earlier prediction times (i.e., $t = 0$), LT-JM begins to surpass RT-JM as prediction time progresses (starting from $t = 2$). This shift is due to the growing availability of longitudinal measurements data but decreasing availability of recurrent CV events information (as fewer patients remain in the study over time). These findings highlight the complementary roles of recurrent and longitudinal data in joint modeling frameworks, particularly in improving the accuracy of competing-risk terminal outcome predictions.

5 Simulation Studies

Simulation studies were conducted to evaluate the performance of the proposed estimation and dynamic prediction procedures and to compare the proposed BM-JM with three marginal models (L-M, R-M, and T-M) and two simplified joint models (LT-JM and RT-JM). The performance of the proposed estimators was assessed using bias, mean-squared error (MSE), and coverage probabilities (CP) of 95% credible intervals (CIs). Simulation results, based on 200 Monte Carlo runs, are summarized in Table S7 and Table S8 of the Supplementary Materials, with detailed simulation setups provided in Appendix E of the Supplementary Materials. The results in Table S7 demonstrate that the BM-JM achieves low bias and MSE values across all parameters in the longitudinal, recurrent, and competing-risk terminal submodels, with CPs consistently close to the expected 95%, underscoring the robustness of the proposed estimation and inference procedure. In contrast, the three marginal models (L-M, R-M, and T-M with results summarized in Table S8) and the two simplified joint models (LT-JM and RT-JM with results summarized in Table S7) exhibited larger biases, particularly in the competing-risk terminal submodels. Additionally, the efficacy of inference using CIs for the competing-risk terminal submodels was notably compromised in all comparative models. These findings emphasize the necessity of caution when interpreting results derived from simpler models.

The proposed dynamic prediction algorithm was also evaluated in simulation studies, with results based on 200 testing datasets reported in Table S9 of the Supplementary Materials. The Dynamic AUC and BS reported for BM-JM demonstrate commendable predictive accuracy across different settings, with all AUC values exceeding 0.74 and BS values falling below 0.20. Additionally, with a fixed follow-up time t and an increasing prediction time window Δt, dynamic AUC values tend to decrease, while dynamic BS values tend to increase, similar to findings reported in predictions of the CRIC data. Furthermore, prediction accuracy does not necessarily improve with increasing time t, despite the availability of more longitudinal measurements and recurrent CV events information. As explained in the CRIC data analysis results, this phenomenon can be attributed to the fact that while there is a reduction in the degree of shrinkage in the estimation of the random effects over time, there is also greater variability in the estimated hazard functions as the prediction time progresses, due to fewer subjects remaining in the study. Finally, similar to the CRIC study findings, the LT-JM and RT-JM models consistently exhibit lower dynamic AUC values and higher dynamic BS values compared to the proposed BM-JM across all settings. The performance gains of the BM-JM are particularly pronounced in later periods, where additional information from recurrent events and longitudinal measurements becomes available. These results underscore the importance of incorporating both longitudinal biomarker and recurrent event data into joint modeling frameworks to enhance predictive accuracy.

6 Discussion

Contributions of this work are multifold. First, the proposed BM-JM addresses the methodological gap in multivariate joint modeling of longitudinal trajectories, recurrent events and competing-risk terminal events, while also providing an efficient dynamic prediction framework for competing-risk terminal outcomes utilizing the combined history of longitudinal measurements and recurrent events. A unique feature of the proposed BM-JM is the explicit modeling of the effects of longitudinal biomarker in the competing-risk survival submodels, allowing for direct quantification and interpretation of the predictive value of the longitudinal measurements on competing-risk terminal outcomes. In addition, the proposed framework allows for prediction of each competing risk individually, leveraging complete longitudinal profile and recurrent events information over time, enhancing predictive accuracy of BM-JM significantly. Dynamic prediction framework provides clinicians with evidence-based insights into the prognostic implications associated with changes in a patient's disease condition.

Additionally, our work, directly motivated by the primary goals of the CRIC study, offers unique findings on CKD progression. The analysis includes the study of the complex network of risk factors influencing key interrelated multivariate outcomes of kidney disease progression, recurrent hospitalizations due to CV events and the eventual competing-risk terminal events of ESKD and death. Dynamic predictions of ESKD and death can serve as an early warning system, offering clinicians valuable lead time to plan and implement interventions effectively. Findings highlight the strong associations between longitudinal eGFR trajectories and ESKD, and recurrent CV events and mortality and hence the importance of considering both longitudinal measurements and recurrent events data in prognostic modeling for CKD patients, as they provide complementary insights into disease progression and outcomes. Finally, the flexibility of our proposed estimation and prediction procedure, developed within a competing risk framework in a Bayesian paradigm, allows for its adaptation to complex scenarios. While our illustration concentrates on one longitudinal, one recurrent and two competing-risk terminal processes, the proposed framework can easily be extended to more intricate situations, including multiple longitudinal biomarkers and more than two competing-risk terminal processes.

While the current joint model employs a linear structure for the longitudinal biomarker, it can be generalized to account for non-linear effects of time if the data suggest such patterns, including higher-order polynomials (e.g., t^2), splines, or other non-linear functions of time. Additionally, exploring alternative noise distributions, such as the extreme value distribution, could provide further insights into model behavior. Although these extensions are beyond the primary scope of this study, they offer promising directions for future research. Moreover, variational Bayes inference (VBI) has gained significant attention in the context of complex machine learning and statistical models for its ability to efficiently approximate posterior distributions. While the complexity of our current model can be adequately handled using the standard MCMC approach, we acknowledge the potential of VBI as a valuable future direction, especially in scenarios with increased computational demands or further model extensions.

Supplementary Material

The online Supplementary Materials include detailed descriptions of the prior distributions and the MCMC implementation used, along with Monte Carlo simulation procedures for estimating $\pi_p^{(w)}(t, s)$. It also includes metrics used to measure dynamic prediction accuracy, the formulations of the comparative models, and an overview of the simulation study setup. Additionally, the

R code and documentation for implementing the proposed BM-JM on simulated datasets are available on Github at https://github.com/dsenturk/BM-JM.

Acknowledgement

The CRIC study is conducted by the CRIC Study Investigators and supported by the National Institute of Diabetes and Digestive and Kidney Diseases (NIDDK). The data from the CRIC study reported here were supplied by the NIDDK Central Repository (https://repository.niddk.nih.gov/home/). This manuscript was not prepared in collaboration with investigators of the CRIC study and does not necessarily reflect the opinions or views of the CRIC study, the NIDDK Central Repository, or the NIDDK. The content reported here is solely the responsibility of authors and does not necessarily reflect the official views of the National Institutes of Health.

Funding

This study was supported by NIDDK grant R01 DK092232 (DS, DVN, EK, SB, CMR, and QQ).

References

Albert PS, Shih JH (2010). An approach for jointly modeling multivariate longitudinal measurements and discrete time-to-event data. *Annals of Applied Statistics*, 4(3): 1517. https://doi.org/10.1214/10-AOAS339

Consortium CKDP et al. (2010). Association of estimated glomerular filtration rate and albuminuria with all-cause and cardiovascular mortality in general population cohorts: A collaborative meta-analysis. *The Lancet*, 375(9731): 2073–2081. https://doi.org/10.1016/S0140-6736(10)60674-5

Coresh J, Selvin E, Stevens LA, Manzi J, Kusek JW, Eggers P, et al. (2007). Prevalence of chronic kidney disease in the United States. *JAMA*, 298(17): 2038–2047. https://doi.org/10.1001/jama.298.17.2038

Eilers PH, Marx BD (1996). Flexible smoothing with b-splines and penalties. *Statistical Science*, 11(2): 89–121. https://doi.org/10.1214/ss/1038425655

Feldman HI, Appel LJ, Chertow GM, Cifelli D, Cizman B, Daugirdas J, et al. (2003). The chronic renal insufficiency cohort (cric) study: Design and methods. *Journal of the American Society of Nephrology*, 14(S2): S148–S153. https://doi.org/10.1097/01.ASN.0000070149.78399.CE

Fine JP, Gray RJ (1999). A proportional hazards model for the subdistribution of a competing risk. *Journal of the American Statistical Association*, 94(446): 496–509. https://doi.org/10.1080/01621459.1999.10474144

Go AS, Chertow GM, Fan D, McCulloch CE, Hsu Cy (2004). Chronic kidney disease and the risks of death, cardiovascular events, and hospitalization. *The New England Journal of Medicine*, 351(13): 1296–1305. https://doi.org/10.1056/NEJMoa041031

Grams ME, Chow EK, Segev DL, Coresh J (2013). Lifetime incidence of ckd stages 3-5 in the United States. *American Journal of Kidney Diseases*, 62(2): 245–252. https://doi.org/10.1053/j.ajkd.2013.03.009

Gueorguieva R, Rosenheck R, Lin H (2012). Joint modelling of longitudinal outcome and interval-censored competing risk dropout in a schizophrenia clinical trial. *Journal of the Royal Statis-*

tical Society. Series A. Statistics in Society, 175(2): 417–433. https://doi.org/10.1111/j.1467-985X.2011.00719.x

Hillege HL, Nitsch D, Pfeffer MA, Swedberg K, McMurray JJ, Yusuf S, et al. (2006). Renal function as a predictor of outcome in a broad spectrum of patients with heart failure. *Circulation*, 113(5): 671–678. https://doi.org/10.1161/CIRCULATIONAHA.105.580506

Jullion A, Lambert P (2007). Robust specification of the roughness penalty prior distribution in spatially adaptive Bayesian p-splines models. *Computational Statistics & Data Analysis*, 51(5): 2542–2558. https://doi.org/10.1016/j.csda.2006.09.027

Kahaner D, Moler C, Nash S (1989). *Numerical Methods and Software*. Prentice-Hall, Inc.

Król A, Ferrer L, Pignon JP, Proust-Lima C, Ducreux M, Bouché O, et al. (2016). Joint model for left-censored longitudinal data, recurrent events and terminal event: Predictive abilities of tumor burden for cancer evolution with application to the ffcd 2000–05 trial. *Biometrics*, 72(3): 907–916. https://doi.org/10.1111/biom.12490

Kürüm E, Kwan B, Qian Q, Banerjee S, Rhee CM, Nguyen DV, et al. (2024). A bayesian joint model of longitudinal kidney disease progression, recurrent cardiovascular events, and terminal event in patients with chronic kidney disease. *Statistics in Biosciences*, https://doi.org/10.1007/s12561-024-09429-6

Lawrence Gould A, Boye ME, Crowther MJ, Ibrahim JG, Quartey G, Micallef S, et al. (2015). Joint modeling of survival and longitudinal non-survival data: Current methods and issues. *Statistics in Medicine*, 34(14): 2181–2195. https://doi.org/10.1002/sim.6141

Liu L, Huang X (2009). Joint analysis of correlated repeated measures and recurrent events processes in the presence of death, with application to a study on acquired immune deficiency syndrome. *Journal of the Royal Statistical Society. Series C. Applied Statistics*, 58(1): 65–81. https://doi.org/10.1111/j.1467-9876.2008.00641.x

Muntner P, He J, Hamm L, Loria C, Whelton PK (2002). Renal insufficiency and subsequent death resulting from cardiovascular disease in the United States. *Journal of the American Society of Nephrology*, 13(3): 745–753. https://doi.org/10.1681/ASN.V133745

Ren X, Wang J, Luo S (2021). Dynamic prediction using joint models of longitudinal and recurrent event data: A Bayesian perspective. *Biostatistics & Epidemiology*, 5(2): 250–266. https://doi.org/10.1080/24709360.2019.1693198

Rizopoulos D (2011). Dynamic predictions and prospective accuracy in joint models for longitudinal and time-to-event data. *Biometrics*, 67(3): 819–829. https://doi.org/10.1111/j.1541-0420.2010.01546.x

Skupien J, Warram JH, Smiles AM, Stanton RC, Krolewski AS (2016). Patterns of estimated glomerular filtration rate decline leading to end-stage renal disease in type 1 diabetes. *Diabetes Care*, 39(12): 2262–2269. https://doi.org/10.2337/dc16-0950

Thiébaut R, Jacqmin-Gadda H, Babiker A, Commenges D, Collaboration C (2005). Joint modelling of bivariate longitudinal data with informative dropout and left-censoring, with application to the evolution of cd4+ cell count and hiv rna viral load in response to treatment of hiv infection. *Statistics in Medicine*, 24(1): 65–82. https://doi.org/10.1002/sim.1923

USRDS (2022). United States Renal Data System 2022 Annual Data Report: "Epidemiology of Kidney Disease in the United States". *Technical report*, National Institutes of Health, National Institute of Diabetes and Digestive and Kidney Diseases, Bethesda, MD.

Williamson PR, Kolamunnage-Dona R, Philipson P, Marson AG (2008). Joint modelling of longitudinal and competing risks data. *Statistics in Medicine*, 27(30): 6426–6438. https://doi.org/10.1002/sim.3451

Wulfsohn MS, Tsiatis AA (1997). A joint model for survival and longitudinal data measured with error. *Biometrics*, 53(1): 330–339. https://doi.org/10.2307/2533118

Yang W, Xie D, Anderson AH, Joffe MM, Greene T, Teal V, et al. (2014). Association of kidney disease outcomes with risk factors for ckd: Findings from the chronic renal insufficiency cohort (cric) study. *American Journal of Kidney Diseases*, 63(2): 236–243. https://doi.org/10.1053/j.ajkd.2013.08.028